Calibration beads containing luminescent lanthanide ion complexes

Robert C. Leif
Sean Yang
Newport Instruments
5648 Toyon Road
San Diego, California 92115-1022

Dayong Jin
James Piper
Macquarie University
Centre for Lasers and Applications
New South Wales 2109, Australia

Lidia M. Vallarino
John W. Williams
Virginia Commonwealth University
Department of Chemistry
Richmond, Virginia 23284-2006

Robert M. Zucker
Environmental Protection Agency
Office of Research and Development
National Health and Environmental Effects Laboratory
Reproductive Toxicology Division
Research Triangle Park, North Carolina 27711

Abstract. The reliability of lanthanide luminescence measurements, by both flow cytometry and digital microscopy, would be enhanced by the availability of narrowband emitting, UV excited lanthanide calibration beads. 0.5-, 3-, and 5-μm beads containing a luminescent europium-complex are manufactured. The luminescence distribution of the 5-μm beads is measured with a time-delayed light-scatter-gated luminescence flow cytometer to have a 7.0% coefficient of variation (CV) The spacial distribution of the europium-complex in individual beads is determined to be homogeneous by confocal microscopy. Emission peaks are found at 592, 616 (width 9.9 nm), and 685 nm with a PARISS® spectrophotometer. The kinetics of the luminescence bleaching caused by UV irradiation of the 0.5- and 5-μm beads measured under LED excitation with a fluorescence microscope indicate that bleaching does not interfere with their imaging. The luminescence lifetimes in water and air were 340 and 460 μs, respectively. Thus, these 5-μm beads can be used for spectral calibration of microscopes equipped with a spectrograph, as test particles for time-delayed luminescence flow cytometers, and possibly as labels for macromolecules and cells. [DOI: 10.1117/1.3103646]

Keywords: luminescence; beads; lanthanide; europium; digital microscopy; standard; spectra; time delayed.

Paper 08211R received Jul. 5, 2008; revised manuscript received Jan. 20, 2009; accepted for publication Jan. 23, 2009; published online Apr. 14, 2009. This paper is a revision of a paper presented at the SPIE conference on Imaging, Manipulation, and Analysis of Biomolecules, Cells, and Tissues VI, January 2008, San Jose, California. The paper presented there appears (unrefereed) in SPIE Proceedings Vol. 6859.

1 Introduction

Many of the steps in the development of an optical instrument, including those employed to optimize its performance, need calibration particles. The europium-complex labeled beads described here have been employed as standard particles to characterize and calibrate instruments, such as a time-gated luminescence (TGL) flow cytometer,[1] a TGL microscope,[2–4] and a microspectrofluorometer.[5] Conversely, the development of a standard material, such as luminescent beads, requires instruments to obtain their spectra and measure the emission intensity of individual beads. The previously described[1] TGL flow cytometer was modified to permit the use of a light-scatter gate. Although numerous types of fluorescent beads are available, the choice of narrowband emitting beads is limited. The development of the europium-complex labeled beads by Newport Instruments was based on requests by collaborators. Example characterizations by these collaborators and by the manufacturer's laboratory are described next.

Address all correspondence to: Robert Leif, R&D, Newport Instruments, 5648 Toyon Road, San Diego, CA 92115. Tel: 619–582–0437; Fax: 619–501–1953; E-mail: rleif@rleif.com.

2 Materials and Methods

2.1 *Starting Materials*

2.1.1 *Europium calibration beads*

The prototype Fire Red™ beads from Newport Instruments (www.newportinstruments.com) were aqueous suspensions of europium-complex of thenoyltrifluoroacetonate (TTFA) labeled polystyrene microspheres (beads), which showed low aggregation and were fairly uniform in size.[6] The beads contained Eu^{3+} coordination complexes, which have an excitation maximum at approximately 370 nm and emit in a narrow region at about 620 nm. Other properties are described in the results in Sec. 3. Before each flow cytometry operation, the sample was ultrasonicated in a water bath to remove particle aggregation.

2.2 *Solutions*

Suspension solution was 0.5% sodium dodecyl sulfate (SDS) with 0.05% sodium azide in distilled water.

1083-3668/2009/14(2)/024022/7/$25.00 © 2009 SPIE

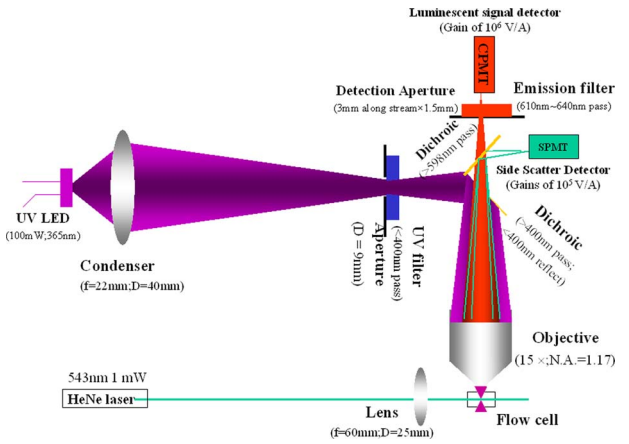

Fig. 1 Drawing describing the optics of the light-scatter-gated time-delayed luminescence flow cytometer. The terms channel photomultiplier tube emission detector and silicon photomultiplier tube have been abbreviated respectively as CPMT and SPMT. (Color online only).

2.3 *Methods*

2.3.1 *Time-gated luminescence flow cytometer*

The details on both concepts[7] and prototype operation[1,8,9] of the time-gated luminescence (TGL) flow cytometer were reported previously. For this work, a TGL flow cytometer was constructed to operate in scatter-triggering TGL mode to ensure that each TGL event received the full 100 μs of UV LED pulse. To improve the precision of the luminescence measurements, a 3-mm (along flow stream) observation aperture was positioned in front of the detector to define a TGL detection spot within a 200-μm-long section of the flow stream, so that when TGL events in the flow stream traveling at 3.2 m/s produce only a 62-μs signal pulse period of the long-lifetime luminescence, which can be detected no matter how long the TGL detector will be on in each scatter-triggered TGL cycle. As shown in Fig. 1, the new system employs the side-scatter channel to trigger the UV LED excitation pulses. As described in Fig. 2, each TGL event will receive uniform excitation for the full 100 μs from each UV LED pulse, and has a constant detection gate width of 62 μs, so that this system is capable of accurately measuring the europium-complex content of each bead.

In Fig. 1, the 543-nm (green) laser and its narrowly focused light emission are shown at the bottom left. A silicon photomultiplier (SPMT) detector (SPMMini100, SensL, www.sensl.com) was positioned after a dichroic mirror (5914C, New Focus, www.newfocus.com) (>598-nm pass, <598-nm reflect) for detection of the side-scattered laser light. The europium-labeled beads were conventionally delivered to the flow cell by a hydrodynamically focused, upflowing laminar stream[8,9] at 3.2 m/s in a single bead profile. The beads were excited by UV light (365 nm) pulses and the red emissions were detected using episcopic fluorescence optics. The scatter signal triggered the UV LED shown at the left [Nichia Model NCCU033A (http://www.nichia.com)], which was focused to generate a 530×530-μm illumination spot with ~15-mW peak power on the sample stream, and remained on for 100 μs. After the LED was extinguished and a subsequent delay of 10 μs, the channel photomultiplier tube (CPMT) emission detector was turned on until the next TGL cycle. This CPMT (MH 1372; PerkinElmer Optoelectronics, Germany) can provide a photon-electron gain as high as 10^6.

Since the lifetime of the europium emission (340 μs) is very long compared to that of conventional organic fluoro-

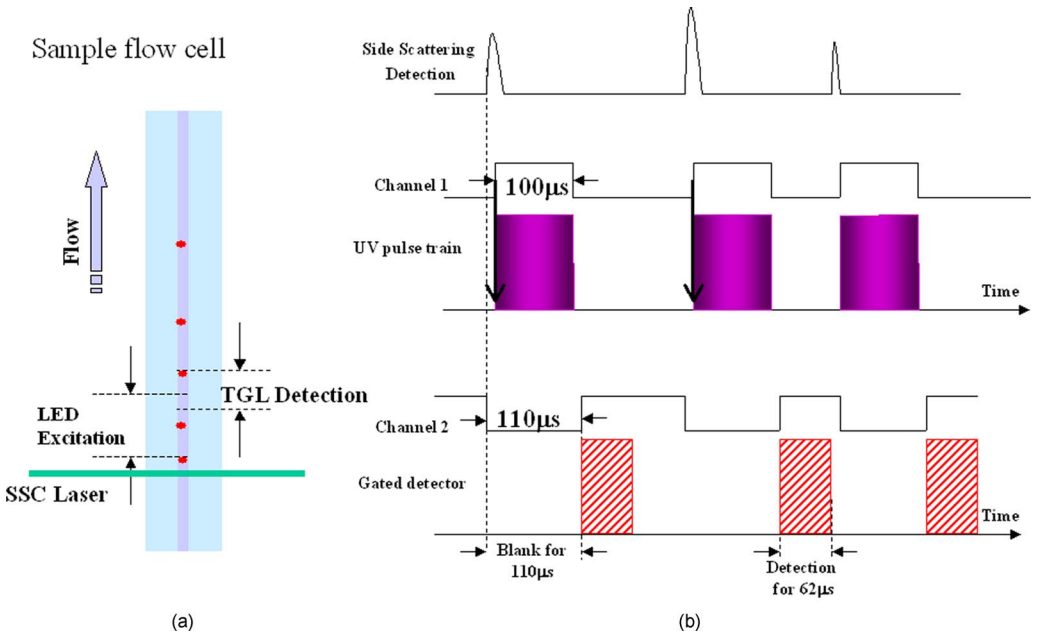

Fig. 2 Drawing that describes the timing of the excitation and detection of the side-scatter and the emission from the light-scatter-gated configuration of a time-gated luminescence (TGL) flow cytometer. (a) shows the upward flow. The small red dots are europium labeled beads or cells. The side scatter (SSC) laser is upstream of the excitation and detection zones, which partially overlap each other. (b) shows from top to bottom respectively the side-scatter triggering pulses, the UV excitation pulses, and the emission detector gates. (Color online only).

phores (nanoseconds), the 10-μs time-resolving period between the extinction of the UV light and the start of the emission acquisition ensures that the background autofluorescence has decreased to being negligible; whereas the luminescence signal from the beads loses little of its original intensity and continues as the bead progresses upstream in the detection area.

2.3.2 *Time-gated luminescence microscopic imaging*

The variation of luminescence intensity amongst individual beads was recorded by imaging the beads under UV LED excitation with a luminescence microscope.[3,4] Images were obtained with essentially continuous excitation from a Nichia UV LED, model No. NCCU033 (http://www.nichia.com). According to the manufacturer's specifications, the emission peak wavelength, half-width, and maximum optical power output were 365 nm, 10 nm, and 100 mW, respectively. A Laserlab power supply (http://www.laserlab.com/) was used to drive the LED in pulsed mode. One millisecond-wide pulses were delivered at 1000 Hz to power the LED. The LED was positioned[3] close to the back of a Linos condenser (16/21.4 mm) (part 06 3010, http://www.linos-photonics.com), which was attached to the excitation entrance of the epi-illuminator of a modified Leitz MPV II fluorescence microscope. The emitted light traversed an Omega Optical (https://www.omegafilters.com/) PloemoPak cube UV DAPI, equipped with a 365-nm narrow bandwidth excitation filter (Omega 365HT25) and a 400-nm beamsplitter (Omega 400DCLP02). The optical path of the CCD was equipped with a 619 nm narrow-band emission filter (Omega 618.6NB.6).

2.3.3 *Charge-coupled device camera*

Images were obtained with a Peltier cooled, monochrome Quantitative Imaging Corporation (http://www.qimaging.com) Retiga-1350 EX, 12-bit ADC, charge-coupled device (CCD) camera (1280×1024). According to the manufacturer's specification, this camera operates at 25 °C below ambient temperature, or ca. 0 °C. The gray levels of the images were inverted for display. Darkness indicates strong luminescence.

2.3.4 *Image analysis*

The image has not been corrected for the inhomogeneous illumination provided by the UV LED. To calibrate the time-gated luminescence intensity from each particle, the intensities were analyzed using ImageJ software (http://rsb.info.nih.gov/ij/). Specifically, the software segmented each target bead by thresholding, the intensity values of each pixel within the threshold-defined area (bead) was integrated, and a histogram was generated from the integrated intensities from each bead. Due to the difficulty in calculating emission intensities from the overlapping particles, all overlapping particles and partially imaged particles from the original image were omitted.

2.3.5 *Image manipulation*

The TIFF images produced by the Retiga-1350 EX camera were manipulated with Adobe® (www.adobe.com) Photoshop® 7.0. All images were transformed into 8-bit grayscale and inverted to facilitate visualization. The conversion of a white image on black background to a black image on white background produces the equivalent of a conventional absorbance image of stained particles or cells. This format was preferred because it is familiar to pathologists and their staff. Other manipulations of 8- or 16-bit images were performed with Fovea (Reindeer Games, Inc. http:// www.reindeer-graphics.com).

2.3.6 *Spectral imaging*

Two microliters of the bead suspension were mixed with a drop of Prolong (Invitrogen) and covered with a 1.5-cm coverglass. A PARISS[5,10–13] (http://www.lightforminc.com) spectral imaging system was connected to a finite Nikon E-800 upright microscope. The spectra of the individual beads were obtained using a 60× Plan Apo (NA 1.4). The DAPI excitation cube (Chroma 31000) (http://www.chroma.com) was used with the emission filter removed.

The machine was tested for accuracy using the multi-ion discharge (MIDL) lamp, which is an inexpensive, eye-safe, battery operated, multi-ion discharge lamp (http://www.lightforminc.com) with defined emission peaks representing mercury (Hg^+), argon (Ar^+), and a fluorophore gas, and tube coating was used as an absolute reference light source because it emits stable, reproducible, peaks between 400 and 650 nm. The lamp was shown to have the following peaks representing Hg: 404.7, 435.7, 546, and 578. The following peaks represent a fluorophore: 485, 544, 586, and 611. The position and shape of each curve represents a signature that all spectroscopic equipment should reproduce. The lamp is simply positioned on the microscope stage above (or below) the objective lens. The characteristics of an acquired spectrum enable the measurements of wavelength accuracy, spectral sensitivity, contrast, wavelength ratios, and spectral resolution. The lamp is used to compare the performance of one instrument over time or against another similar instrument at a different location.

The wavelength of the mode (maximum) of the major emission peak from the beads was estimated as being halfway between those of the two highest recorded values, which had approximately the same amplitude. The shift in the maximum of the major emission peak was determined from a nonparametric statistic, the truncated median. A distribution of the summed emission values was calculated, starting with the first data point with a value above the minimum of the major peak (blue side) of the spectrum, and ending with the first data point with a value above the minimum on the long-wavelength (infrared side). The truncated medium of the major peak was then determined by linear interpolation between the values of two adjacent values of the summed distribution. The first value was less than, and the second greater than, one-half of the maximum (last) value of the summation. The fractional value produced by the interpolation was added to the wavelength of the first value.

2.3.7 *Confocal microscopy*

The beads were prepared as described in Sec. 2.3.6. Images of the inside of the bead were obtained with a Leica TCS-SP1 Confocal Spectral Imaging (CSI) Microscope System, which includes an argon-krypton laser (Melles Griot, Omnichrome), which emits lines at 488, 568, and 647 nm, and a Coherent

Enterprise UV laser, which emits lines at 351 and 365 nm. Excitation light from the UV laser was delivered to the specimen with a 70/30 reflector and a PlanApo 63×1.32-NA objective. The scan rate was set to slow to permit detection of the long-lived emission of the europium-complex. Spectral scans were acquired with a 5-nm bin size. The Leica SP1 measures spectra between 430 and 725 nm with 5-nm bin widths. The CSI systems were operated with an Airy disk of 1. Electronic zoom was set to 4.

The data from intensity scans (histograms) from two adjacent lines near the center of a bead were transferred to Microsoft Excel and graphed. Since there was an obvious shift in position, the second spectrum was shifted until it overlaid the first. The average difference between matching points of the two scans was virtually unchanged by movement of one relative to the other in a range of 30 pixels out of 1047.

2.3.8 *Lifetime measurements*

The luminescence lifetimes of the europium labeled beads were measured with the custom-built TGL fluorometer. In the epi-illumination optics, a Nichia 100-mW UV LED was used to generate pulsed UV excitation at 365 nm. The europium emission was finally filtered by an aperture and a bandpass filter [Pass-band Center 624 nm; full width at half maximum (FWHM) ~30 nm; model 5914-B, New Focus, http://www.newfocus.com]. To detect time-delayed luminescence decay curves, a time-gated high-gain photomultiplier is essential to prevent the intense LED emission from reaching the sensitive photodetector during the excitation phase. For this purpose, a new-generation (engineering sample) silicon photomultiplier tube (SPMT) was supplied by one of our collaborators, SensL Ireland (http://www.sensl.com). This SPMT can provide a photon-electron gain as high as 10^6, as well as a much larger (3×3 mm) sensitivity area. This detector is superior to others for time-gated luminescence sensing applications, because it can be gated easily by controlling a pulsed bias voltage (~30 V) supply, resulting in a rise time as short as 4 μs. The current-voltage preamplifier converted the TGL anode current signal into voltage (500-kHz bandwidth; 104 V/A gain) and the subsequent signal was averaged over 20 cycles on a digital oscilloscope (TDS420; Tektronix Inc. http://www.tek.com). The LED injection current was monitored on a digital oscilloscope (typically 1 A).

2.3.9 *Bleaching studies*

The variation in the rate of UV irradiation-induced photobleaching among individual beads was measured using the luminescence microscope described in Sec. 2.3.2 with the same filters and dichroic mirror. The only change was an increase in excitation intensity due to the use of a new 365-nm UV LED with 200-mW output (Nichia Model NCSU033A). The 3- and 5-μm beads were suspended in 0.5 mL of the suspension solution. Each set of beads was then sonicated twice for 10 sec using a Branson Sonifier (model 450) equipped with a microtip (101-148-062) at 20% amplitude. The beads were then diluted one-to-one with distilled water; a wet mount was then made with 5 μL of the bead suspension, and clear nail polish was applied around the edges of the coverslip to prevent drying. Images were acquired with the Retiga-1350 EX camera. Pseudocontinuous excitation was achieved by providing 1-ms pulses at 1 kHz to the UV LED, using a 40× objective with an NA of 0.65.

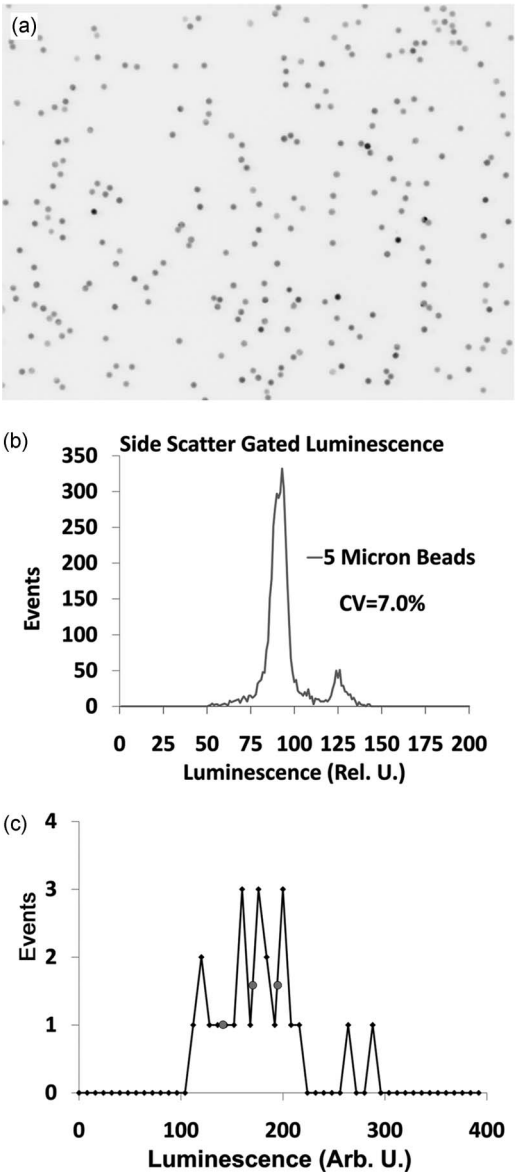

Fig. 3 Newport Instrument's Fire Red 5-μm europium-calibration beads. (a) Luminescence image obtained with a 10×0.25-NA objective with 2×2 binning. The exposure was approximately 1 s. The 200-mw UV LED was used for excitation. The beads are essentially homogeneous except for a few dark ones. The image has been inverted. (b) Luminescence distribution obtained with light-scatter-gated flow cytometer. (c) Luminescence histogram obtained from an image of 24 beads. The three dots ● are located at 25, 50, and 75% of the area of the histogram.

3 Results

3.1 *Quantitative Luminescence Distribution Studies*

A representative image of the 5-μm beads is shown in Fig. 3(a). The luminescence distribution from individual beads was measured with a light-scatter-gated luminescence flow cytometer and by digital microscopy. The 7% CV of these

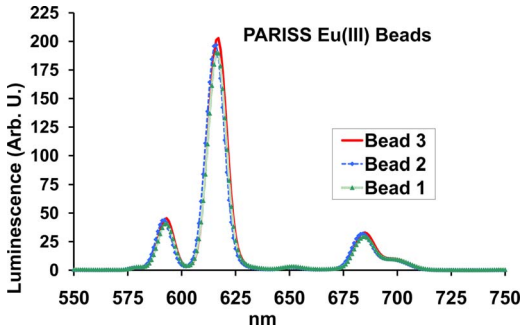

Fig. 4 Europium-complex emission spectrum obtained from three beads (the numbering is arbitrary) using a PARISS spectrometer system. The europium-complex labeled beads were excited with 365-nm light, and the emission was measured between 550 and 750 nm. The PARISS system used a UV cube to excite the beads. The emission resolution was 1 nm. Three spectra were selected that had approximately the same intensity of major peak luminescence. (Color online only).

emissions obtained by light-scatter-gated luminescence flow cytometer [Fig. 3(b)] is in good agreement with the CV (8.0%) of the emission distribution obtained by the time-gated luminescence (TGL) flow cytometer, which is described in the companion publication.[9] Since the distribution obtained by TGL flow cytometry was artificially broadened at the lower values, the CV for the TGL flow cytometer was measured from the higher values. Although the microscopic data shown in Fig. 3(c) is too sparse to fit with a curve, it definitely does not have a tail at lower values and is suggestive of Fig. 3(b).

3.2 *Spectral Imaging Studies*

Figure 4 shows that the europium-complex labeled beads have a well-defined emission at 685 nm, which was not detected with a PMT-based instrument.[14] The numbering of the beads is arbitrary. As shown in Table 1, the mode (maximum) of the most intense peak (616.5 nm) for the three spectra is at 616.5 nm, and the relative position of the three peaks in the

Table 1 Fire Red™ beads, major peaks.

Statistic	Bead 1	Bead 2	Bead 3	Average
Mode	616.5	616.5	616.5	616.5
Width at Half Max	10.0	9.92	9.78	9.9
Truncated Median	616.0	616.1	616.2	616.1

emission histograms is maintained. The truncated medians for the maximum emission by beads differ by approximately 0.2 nm with an average of 616.1 nm. The width at half maximum ranges from 9.8 to 10.0 nm. These data demonstrate that luminescent beads, in combination with a fluorescence microscope equipped with the PARISS instrument, give highly reproducible spectra.

3.3 *Confocal Microscopy of Beads*

Confocal image of the center of a typical individual bead [Fig. 5(a)] demonstrates that the luminescence comes from the bulk of the bead and is not limited to the surface.

As shown in Fig. 5(b), both Scan 2 and Scan 2 (which was offset to be superimposed on scan 1), differ from scan 1. At present, it is not possible to state whether this difference is due to microheterogeneity in the bead luminescence, instrument noise, or both. Future improvements in technique will be required to settle this question. However, the scans and the image do establish the important fact that the luminescence is distributed through the bead and is not just located at the surface. Since luminescence and fluorescence are linear phenomena, their heterogeneity does not significantly affect quantitation.

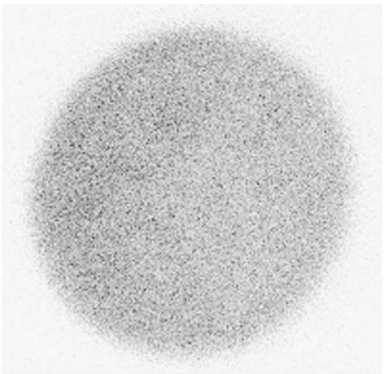

(a)

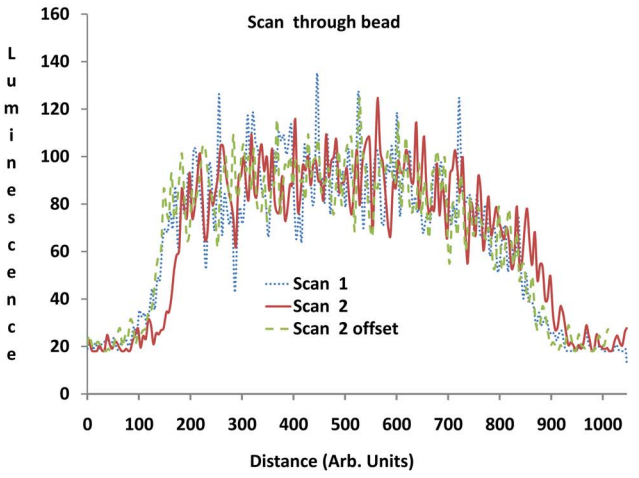

(b)

Fig. 5 (a) shows an inverted monochrome confocal image of the center section of a 5-μm bead and (b) shows two adjacent line scans of the luminescence (arbitrary units) through the center of the image. Scan 2 was offset to try to line it up with scan 1. (Color online only).

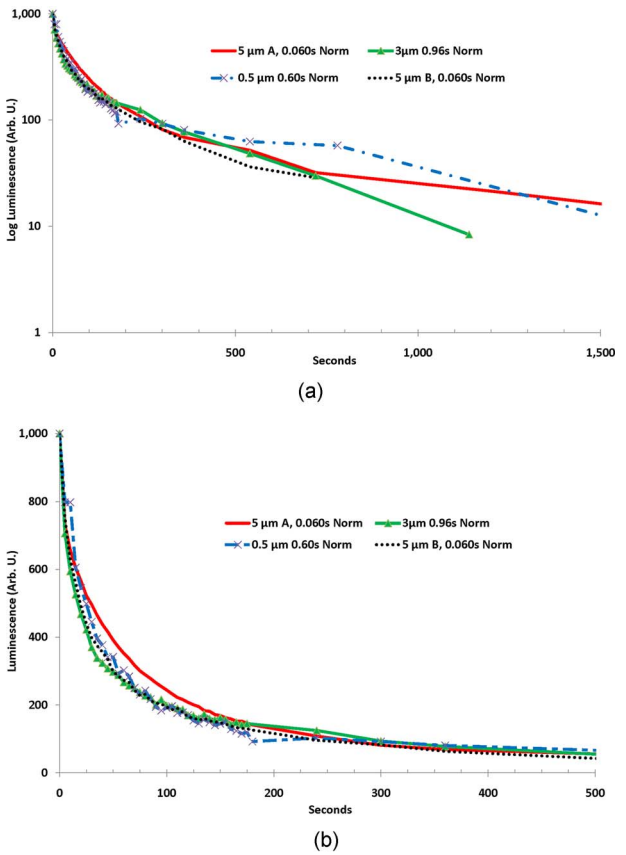

Fig. 6 (a) A logarithmic and (b) linear graph of the same data that illustrate the time dependence of the luminescence bleaching for the 0.5-, 3-, and two 5-μm bead preparations (5 μm A and 5 μm B) upon irradiation at 365 nm. In these experiments, the LED power output through the objective was 1.75 mW (the maximum output was 9.9 mW) and the images were taken at 5-s intervals. The intensities of the emissions were corrected by the ratio of the exposure periods, and the maxima were normalized to 1000. The exposure times of the individual preparations are shown in the legends of the graphs. (Color online only).

3.4 *Ultraviolet Bleaching Studies*

Figure 6 shows that both the logarithmic [Fig. 6(a)] and linear [Fig. 6(b)] plots of luminescence intensity against time demonstrate considerable deviation from linearity in the first decade (1000 to 100 arbitrary units). After the luminescence intensity had decreased approximately one-hundred-fold, the exposure time was increased. Except for the 0.96-s exposures of the 5-μm A beads, the noise predominated.

Figure 6(b) and Table 2 show that the bleaching half-life of

Table 2 Bleaching.

Size μm	0.5	3	5 A	5 B
Half-Life	24.8	17.2	29.3	19.3
Illumination period	0.060	0.960	0.060	0.060
Number of Images	414	18	489	322

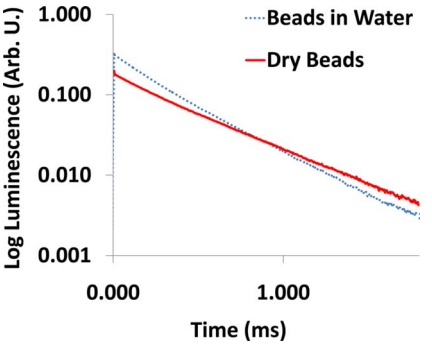

Fig. 7 Luminescence decay lifetime measurements. The slope for the beads in water is greater than that for the dry beads. (Color online only).

the 0.5 μm, 5 μm A, and 5 μm B preparations were 24.8, 29.3, and 19.3 s, respectively. From these values and the common exposure (excitation) period (0.060 s) necessary to obtain an image of these beads, the maximum number of images attainable for the 0.5 μm, 5 A μm, and 5 B μm preparations was calculated to be 414, 489, and 322. For the 3-μm beads, which had a shorter half-life (17.2 s), and which required a 16 times longer illumination period to obtain an image, the maximum number of images attainable was 18. These beads were therefore unsuitable for use, presumably because of a much lower content of the europium-complex. It should be noted that photobleaching does not appear to be a problem, since more than 300 illumination periods were required for the luminescence intensities of the 0.5-μm and of the two 5-μm bead preparations to decrease to one-half of their initial values. Longer bleaching half-lives would be expected for dry or nonaqueous slide preparations.

3.5 *Luminescence Lifetime Studies*

The luminescence lifetimes (t1) calculated from the data shown in Fig. 7 for the dry beads and for the beads in water were respectively 460 ± 1.2 μs and 340 ± 1.1 μs. This difference can be ascribed to luminescence quenching by the solvent suspending fluid, water, of the beads in water.

4 Conclusions

The results reported in the accompanying publication[9] show that the count of 5-μm beads can be detected quantitatively using a time-delayed luminescence flow cytometer,[1,8,9] even in samples with a high fluorescence background. Homogeneously labeled luminescent europium-complex labeled beads have been prepared that are suitable for research uses, such as microspectrophotometer and luminescence flow cytometer standardization. The europium-complex labeled beads provide the great value of having well-defined, reproducible emission peaks and small full widths at half maximum. The narrow bandwidth and highly reproducible red emissions of these beads are critical for the detection and quantitation of probes (i.e., CY 7 or Draq 5) that fluoresce in the 650- to 800-nm range. The photobleaching of these beads is a complex phenomenon that appears to be independent of size, but probably does depend on the composition of the beads. The homogeneous distribution of the europium-complex in the beads, lack

of concentration quenching, and the fact that reducing the size of the beads does not increase their fading rate should permit the development of very sensitive labels for macromolecules and cells. These labels have the significant advantage over quantum dots of having a much higher number of labels per unit volume.

There is a circular relationship between precision instruments and standard materials; each needs the other. This circle will be completed by the availability of reliable lanthanide calibration beads, which in turn facilitates appropriate modifications to precision instruments, such as the TGL luminescence flow cytometer, that permit accurate quantitation of the luminescence intensity of individual beads.

Acknowledgments

The authors wish to acknowledge the Australian ARC/NHMRC FABLS (Fluorescence Applications in Biotechnology and Life Sciences) network for a seeding project fund to support emerging new technology, the ISAC (International Society for Analytical Cytology) scholar program, the National Natural Science Foundation of China (number 20575069), Newport Instruments' Internal Development Funds, and Lidia Vallarino's Gift Fund. Robert C. Leif and Sean Yang are employees of Newport Instruments, which is the supplier of the Fire-Red™ beads. This work has been reviewed and approved for publication as an EPA document. Approval does not necessarily signify that the contents reflect the views and policies of the agency, nor does mention of trade names or commercial products constitute endorsement or recommendation for use.

References

1. D. Jin, R. Connally, and J. Piper, "Practical time-gated luminescence flow cytometry. II: experimental evaluation using UV LED excitation," *Cytometry, Part A* **71A**, 797–808 (2007).
2. R. C. Leif, M. C. Becker, L. M. Vallarino, J. W. Williams, and S. Yang, "Progress in the use of Quantum Dye® Eu(III)-macrocycles," *Proc. SPIE* **4962**, 341–353 (2003).
3. R. C. Leif, L. M. Vallarino, M. C. Becker, and S. Yang, "Increasing lanthanide luminescence by use of the RETEL effect," *Cytometry, Part A* **69A**, 940–946 (2006).
4. R. Connally, D. Jin, and J. Piper, "High intensity solid-state UV source for time-gated luminescence microscopy," *Cytometry, Part A* **69A**, 1020–1027 (2006).
5. J. L. Lerner and R. M. Zucker, "Calibration and validation of confocal spectral imaging systems," *Cytometry, Part A* **61A**, 8–34 (2004).
6. R. C. Leif, D. Jin, J. A. Piper, L. M. Vallarino, J. W. Williams, S. Yang, and R. M. Zucker, "Lanthanide ion containing calibration beads," *Proc. SPIE* **6859**, 685917 (2008).
7. D. Jin, R. Connally, and J. Piper, "Practical time-gated luminescence flow cytometry," *Cytometry, Part A* **71A**, 783–796 (2007).
8. D. Jin, B. Ferrari, R. C. Leif, S. Yang, L. M. Vallarino, J. W. Williams, and J. Piper, "UV LED excited time-gated luminescence flow cytometry: evaluation for rare-event particle counting," *Proc. SPIE* **6859**, 68590O (2008).
9. D. Jin, J. Piper, R. C. Leif, S. Yang, B. C. Ferrari, J. Yuan, G. Wang, L. M. Vallarino, and J. W. Williams, "Time-gated luminescence flow cytometry: an ultra-high selectivity method to recover ultra-rare-event μ-targets in raw biosamples," *J. Biomed. Opt.* **14**, 024023 (2009).
10. R. M. Zucker and J. L. Lerner, "Wavelength and alignment tests for confocal imaging systems microscopy research and technique," *Cytometry, Part A* **68**, 307–319 (2005).
11. R. M. Zucker and O. T. Price, "Practical confocal microscopy and the evaluation of system performance," *Methods* **18**, 447–458 (1999).
12. R. M. Zucker and O. T. Price, "Evaluation of confocal microscopy system performance," *Cytometry* **44**, 273–294 (2001).
13. R. M. Zucker, P. Rigby, I. Clements, W. Salmon, and P. Chua, "Reliability of confocal spectral imaging systems: use of multispectral beads," *Cytometry, Part A* **71A**, 174–189 (2007).
14. R. C. Leif, L. M. Vallarino, M. C. Becker, and S. Yang, "Increasing the luminescence of lanthanide complexes," *Cytometry, Part A* **69A**, 767–778 (2006).